



# HHS Public Access

Author manuscript

*Chem Biol.* Author manuscript; available in PMC 2023 January 25.

Published in final edited form as:

*Chem Biol.* 2014 November 20; 21(11): 1546–1556. doi:10.1016/j.chembiol.2014.10.004.

## Intracellular Calcium Levels Determine Differential Modulations of Allosteric Interactions within G Protein-Coupled Receptor Heteromers

Gemma Navarro<sup>1,\*</sup>, David Aguinaga<sup>1</sup>, Estefania Moreno<sup>1</sup>, Johannes Hradsky<sup>2</sup>, Pasham P. Reddy<sup>2</sup>, Antoni Cortés<sup>1</sup>, Josefa Mallo<sup>1</sup>, Vicent Casadó<sup>1</sup>, Marina Mikhaylova<sup>2,3</sup>, Michael R. Kreutz<sup>2</sup>, Carme Lluís<sup>1</sup>, Enric I. Canela<sup>1,†</sup>, Peter J. McCormick<sup>1,4,†</sup>, Sergi Ferré<sup>5,\*</sup>,†

<sup>1</sup>Department of Biochemistry and Molecular Biology, Faculty of Biology, University of Barcelona, Centro de Investigación Biomédica en Red Sobre Enfermedades Neurodegenerativas and Institute of Biomedicine of the University of Barcelona (IBUB), Barcelona 08028, Spain;

<sup>2</sup>Research Group Neuroplasticity, Leibniz-Institute for Neurobiology, Magdeburg 39118, Germany;

<sup>3</sup>Cell Biology, Utrecht University, Utrecht 3584CH, The Netherlands;

<sup>4</sup>School of Pharmacy, University of East Anglia, Norwich NR47TJ, United Kingdom.

<sup>5</sup>Integrative Neurobiology Section, National Institute on Drug Abuse, Intramural Research Program, National Institutes of Health, Department of Health and Human Services, Baltimore, Maryland 21224, USA

### SUMMARY

The pharmacological significance of the adenosine A<sub>2A</sub> receptor (A<sub>2A</sub>R)-dopamine D<sub>2</sub> receptor (D<sub>2</sub>R) heteromer is well established and it is being considered as an important target for the treatment of Parkinson's disease and other neuropsychiatric disorders. However, the physiological factors that control its distinctive biochemical properties are still unknown. We demonstrate that different intracellular Ca<sup>2+</sup> levels exert a differential modulation of A<sub>2A</sub>R-D<sub>2</sub>R heteromer-mediated adenylyl-cyclase and MAPK signaling in striatal cells. This depends on the ability of low and high Ca<sup>2+</sup> levels to promote a selective interaction of the heteromer with the neuronal Ca<sup>2+</sup>-binding proteins NCS-1 and calneuron-1, respectively. These Ca<sup>2+</sup>-binding proteins differentially modulate allosteric interactions within the A<sub>2A</sub>R-D<sub>2</sub>R heteromer, which constitutes a unique

\* **Corresponding authors:** Dr. Gemma Navarro, Department of Biochemistry and Molecular Biology, Faculty of Biology, University of Barcelona, Diagonal 645, 08028 Barcelona, Spain; dimarts@hotmail.com; Dr. Sergi Ferré, Integrative Neurobiology Section, NIDA, IRP, Triad Technology Building, 333 Cassell Drive, Baltimore, MD 21224; sferre@intra.nida.nih.gov.

† Co-senior authors

Author contributions

*Research design:* G.N., M.M., M.R.K., A.C., J.M., V.C., C.L., E.I.C., P.J.M., S.F.

*Experiments:* G.N., D.A., E.M., J.H., P.P.R., M.M.

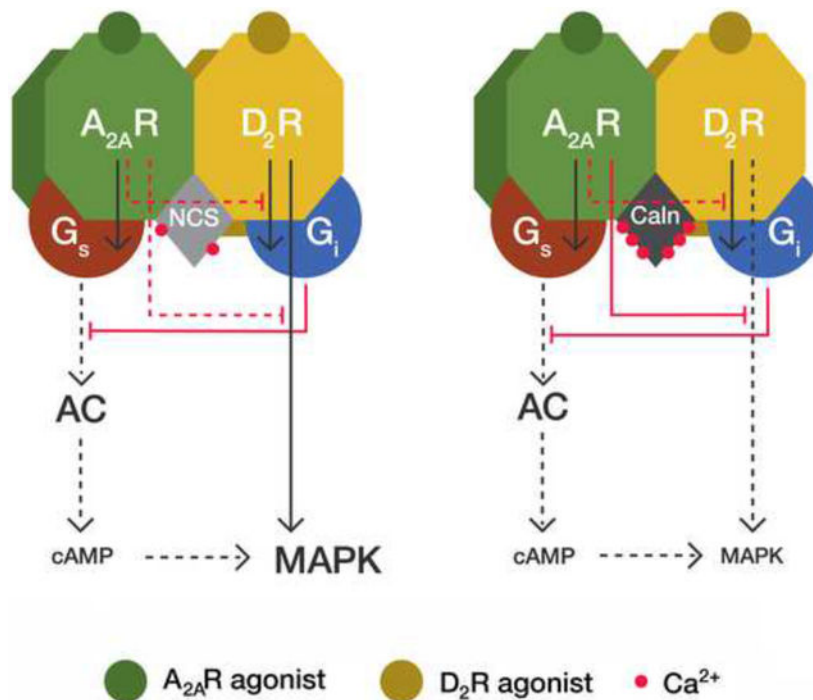
*Data analysis:* G.N., D.A., E.M., J.H., P.P.R., M.M., C.L., P.J.M., S.F.

*Writing of the manuscript:* G.N., M.M., C.L., P.J.M., S.F.

**Publisher's Disclaimer:** This is a PDF file of an unedited manuscript that has been accepted for publication. As a service to our customers we are providing this early version of the manuscript. The manuscript will undergo copyediting, typesetting, and review of the resulting proof before it is published in its final citable form. Please note that during the production process errors may be discovered which could affect the content, and all legal disclaimers that apply to the journal pertain.

cellular device that integrates extracellular (adenosine and dopamine) and intracellular ( $\text{Ca}^{2+}$ ) signals to produce a specific functional response.

### Graphical Abstract



### INTRODUCTION

G-protein coupled receptors (GPCR) heteromers are defined as macromolecular complexes composed of at least two functional receptor units with biochemical properties that are different from those of its individual receptors (Ferré et al., 2009). Allosteric mechanisms are responsible for a multiplicity of unique pharmacological properties of GPCR heteromers (Ferré et al., 2014). One of the most reproduced allosteric modulations in a GPCR heteromer is an antagonistic interaction by which adenosine  $\text{A}_{2\text{A}}$  receptor ( $\text{A}_{2\text{A}}\text{R}$ ) agonists decrease the affinity of dopamine  $\text{D}_2$  receptor ( $\text{D}_2\text{R}$ ) agonists in the  $\text{A}_{2\text{A}}\text{R}$ - $\text{D}_2\text{R}$  heteromer (Ferré et al., 1991).  $\text{A}_{2\text{A}}\text{R}$ - $\text{D}_2\text{R}$  heteromers were one of the first GPCR heteromers detected in the brain. They are localized in the striatum, in the GABAergic striato-pallidal neurons, where they play a seminal role controlling basal ganglia function and dysfunction (Ferré et al., 2011).

Apart from modulation of ligand affinity, GPCR oligomers enable ligands to exert different intrinsic efficacy (power of the agonist to induce a functional response independent of its affinity for the receptor) for different signaling pathways (functional selectivity) (Ferré et al., 2014). Thus, allosteric changes in the functional response of an agonist can be mediated by changes in affinity and/or intrinsic efficacy. This principal can be observed in the  $\text{A}_{2\text{A}}\text{R}$ - $\text{D}_2\text{R}$  heteromer, where a decrease in  $\text{D}_2\text{R}$  agonist affinity could not alone explain the ability of  $\text{A}_{2\text{A}}\text{R}$  agonists to abolish the decrease in excitability of GABAergic striato-pallidal neurons

induced by high concentrations of D<sub>2</sub>R agonists, sufficient to overcome their decreased affinity (Azdad et al., 2009).

A<sub>2A</sub>R and D<sub>2</sub>R couple preferentially to G<sub>s/olf</sub> and G<sub>i</sub> proteins, respectively, and several studies have reported an antagonistic interaction reciprocal to the A<sub>2A</sub>R-D<sub>2</sub>R allosteric modulations, the ability of D<sub>2</sub>R ligands to potently inhibit A<sub>2A</sub>R agonist-mediated adenylyl-cyclase (AC) activation (Kull et al., 1999; Hillion et al., 2002). It is not known if this canonical interaction between G<sub>s</sub>- and G<sub>i</sub>-mediated signaling pathways takes place in the frame of the A<sub>2A</sub>R-D<sub>2</sub>R heteromer, as suggested for dopamine D<sub>1</sub>-D<sub>3</sub> receptor heteromers (Guitart et al., 2014), or if it depends on separate receptor populations (Ferré et al., 2011). But if it is a property of the A<sub>2A</sub>R-D<sub>2</sub>R heteromer, we do not know the physiological factors that modulate these reciprocal interactions, determining the final neuronal response.

Intracellular Ca<sup>2+</sup> levels are a physiological factor that modulates neuronal activity and GPCR function. The Ca<sup>2+</sup>-binding protein calmodulin (CaM) has been shown to interact and modulate A<sub>2A</sub>R and D<sub>2</sub>R function in the A<sub>2A</sub>R-D<sub>2</sub>R heteromers, but without altering the allosteric interactions between A<sub>2A</sub>R and D<sub>2</sub>R ligands (Navarro et al., 2009; Ferré et al., 2010). CaM is an ancestor of a superfamily of Ca<sup>2+</sup>-binding proteins, which includes neuronal members classified in neuronal Calcium Binding Proteins (CaBPs, such as caldendrin and calneuron-1) and the Neuronal Calcium Sensor (NCS) proteins (such as NCS-1) (Mikhaylova et al., 2011). NCS-1, caldendrin and calneuron-1 have overlapping expression in the brain and have been shown to dramatically modify GPCR function (Mikhaylova et al., 2009). NCS-1 is also known to interact and modify the function of A<sub>2A</sub>R and D<sub>2</sub>R (Kabbani et al., 2002; Saab et al., 2009; Navarro et al., 2012). We therefore studied if neuronal Ca<sup>2+</sup>-binding proteins could provide the pursued modulators of the allosteric interactions in the A<sub>2A</sub>R-D<sub>2</sub>R heteromers.

## RESULTS

### NCS-1 and calneuron-1 directly interact with A<sub>2A</sub>R-D<sub>2</sub>R heteromers

Bioluminescence Resonance Energy Transfer (BRET) experiments were performed in HEK-293T cells in which one of the receptors is fused to the bioluminescent protein *Renilla* Luciferase (RLuc) and the Ca<sup>2+</sup>-binding protein to a yellow fluorescent protein (YFP). Protein interactions were detected by saturable BRET curves in cells expressing a constant amount of A<sub>2A</sub>R-Rluc or D<sub>2</sub>R-Rluc and increasing amounts of NCS-1-YFP or calneuron-1-YFP (Figure 1A; top and middle graphs). BRET<sub>max</sub> and BRET<sub>50</sub> values were, respectively: 59.6 ± 4 mBU and 42.4 ± 9 for the pair A<sub>2A</sub>R-Rluc-NCS1-1-YFP; 35.8 ± 4 mBU and 23.4 ± 5 for the pair D<sub>2</sub>R-Rluc-NCS-1-YFP; 118.1 ± 7 mBU and 40.5 ± 7 for the pair A<sub>2A</sub>R-Rluc-calneuron-1-YFP and 51.9 ± 10 mBU and 25.7 ± 7 for the pair D<sub>2</sub>R-Rluc-calneuron-1-YFP. Very low and linear BRET was detected in cells expressing a constant amount of A<sub>2A</sub>R-Rluc or D<sub>2</sub>R-Rluc and increasing amounts of caldendrin-YFP (Figure 1A; bottom graph), showing the inability of caldendrin to interact with A<sub>2A</sub>R or D<sub>2</sub>R, and the specificity of NCS-1 and calneuron-1 interactions. Increase intracellular Ca<sup>2+</sup> levels with ionomycin produced noticeable changes in the BRET curves for the pairs A<sub>2A</sub>R-Rluc-NCS-1-YFP, D<sub>2</sub>R-Rluc-NCS-1-YFP and A<sub>2A</sub>-Rluc-calneron-1-YFP (Figure 1A; top and middle graphs), indicating that Ca<sup>2+</sup> binding to NCS-1 or calneuron-1 induces

structural changes in the respective complexes. In accordance with the BRET data, the intracellular distribution of NCS-1 dramatically changed to a plasma membrane distribution after A<sub>2A</sub>R or D<sub>2</sub>R co-expression (Figure 1B; top panel). Calneuron-1 expressed alone showed a membrane localization that was maintained in the presence of A<sub>2A</sub>R or D<sub>2</sub>R with a high degree of co-localization (Figure 1B; middle panel). Calendrin did not change its intracellular distribution when co-expressed with either receptor (Figure 1B; bottom panel).

Heteromers were detected by saturable BRET curves in cells expressing a constant amount of A<sub>2A</sub>R-Rluc and increasing amounts of D<sub>2</sub>R-YFP in the absence or in the presence of ionomycin (Figure 2A). Co-expression of calneuron-1 or NCS-1 induced structural changes in the heteromer detected as changes in the BRET curve shape (Figure 2A). This suggested oligomerization between A<sub>2A</sub>R-D<sub>2</sub>R heteromers and the Ca<sup>2+</sup>-binding proteins, which was further supported by Sequential Resonance Energy Transfer (SRET) experiments (Carriba et al., 2008). Rluc was fused to A<sub>2A</sub>R to act as a BRET donor, GFP<sup>2</sup> was fused to D<sub>2</sub>R to act as a BRET acceptor and as a FRET donor and YFP was fused to NCS-1 or to calneuron-1 to act as a FRET acceptor as diagrammed in Figure 2B (top scheme). In cells expressing a constant amount of A<sub>2A</sub>R-Rluc and D<sub>2</sub>R-GFP<sup>2</sup> and increasing amounts of NCS-1-YFP (Figure 2B; middle graph) or calneuron-1-YFP (Figure 2B; bottom graph), a positive SRET saturation curve was obtained in the absence (black curves) or in the presence (red curves) of ionomycin, with a SRET<sub>max</sub> of 73.3 ± 2 mSU and SRET<sub>50</sub> of 8.9 ± 2 or SRET<sub>max</sub> of 88.2 ± 9 mSU and SRET<sub>50</sub> of 24.1 ± 6 for the A<sub>2A</sub>R-D<sub>2</sub>R-NCS-1 complex in the absence or in the presence of ionomycin, respectively, and a SRET<sub>max</sub> of 113.2 ± 14 mSU and SRET<sub>50</sub> of 25.1 ± 7 or SRET<sub>max</sub> of 122.6 ± 15 mSU and SRET<sub>50</sub> of 38.5 ± 10 for the A<sub>2A</sub>R-D<sub>2</sub>R-calneuron-1 complex in the absence or in the presence of ionomycin, respectively. Therefore, both NCS-1 and calneuron-1 bind to A<sub>2A</sub>R-D<sub>2</sub>R heteromers independently of the presence of Ca<sup>2+</sup>.

To investigate if membrane localization of the Ca<sup>2+</sup>-binding proteins, mediated by C-terminal transmembrane domain in calneuron-1 and N-terminal myristoylation of NCS-1 (Hradsky et al., 2011), are necessary for the interaction with A<sub>2A</sub>R and D<sub>2</sub>R, we used a calneuron-1 construct truncated in its C terminus (calneuron-1 CT) (Hradsky et al., 2011), and an N-terminal myristoylation-deficient NCS-1 mutant. No BRET signal was detected in cells expressing A<sub>2A</sub>R-Rluc or D<sub>2</sub>R-Rluc and increasing amounts of mutant calneuron-YFP (Figure S1A; top graphs). Very low and linear BRET values were also obtained in cells expressing A<sub>2A</sub>R-Rluc or D<sub>2</sub>R-Rluc and increasing amounts of mutant NCS-1-YFP (Figure S1A; bottom graphs).

### **NCS-1 and calneuron-1 compete for the binding to A<sub>2A</sub>R and D<sub>2</sub>R**

Competition BRET experiments were performed in which energy transfer between A<sub>2A</sub>R-Rluc-NCS-1-YFP was measured in the presence of increasing concentrations of calneuron-1 with or without ionomycin (Figure 3A; left graph). In both conditions, calneuron-1 dose-dependently lowered the energy transfer, indicating competition between both Ca<sup>2+</sup> binding proteins for A<sub>2A</sub>R. Similar results were obtained with D<sub>2</sub>R. NCS-1 reduced the energy transfer between D<sub>2</sub>R-Rluc and calneuron-1-YFP in the absence or presence of ionomycin (Figure 3A; right graph). Therefore NCS-1 and calneuron-1 bind and compete for the same

binding sites on A<sub>2A</sub>R and D<sub>2</sub>R. In agreement, low and linear SRET curves were obtained in the absence or in the presence of ionomycin in cells expressing A<sub>2A</sub>R-Rluc-calneuron-1-GFP<sup>2</sup>-NCS-1-YFP or D<sub>2</sub>R-Rluc-calneuron-1-GFP<sup>2</sup>-NCS-1-YFP (Figure 3B).

BRET saturation values were significantly diminished when a mutant A<sub>2A</sub>R fused to Rluc in which the sequence <sub>199</sub>RIFLAARRQ<sub>207</sub> (localized in the cytoplasm, at the end of TM5) was mutated to <sub>199</sub>RIFLAAAQ<sub>207</sub> (A<sub>2A</sub>R<sup>A205-A206</sup> receptor) was co-expressed with either NCS-1-YFP or calneuron-1-YFP (Figure S1B). NCS-1 and calneuron-1 thus interact with the third intracellular loop (3IL) of A<sub>2A</sub>R. This was confirmed by surface plasmon resonance measurements showing the *in vitro* interaction between the Ca<sup>2+</sup>-binding proteins and GST fused to a peptide with the amino acid sequence corresponding to the third intracellular loop of the A<sub>2A</sub>R (GST-A<sub>2A</sub>R-IL3) (Figure S2; top graphs). The sequence corresponding to amino acids 428–443 in the C-terminal domain of the D<sub>2</sub>R has been involved in NCS-1 binding (Kabbani et al., 2002). In agreement, a complete loss of BRET was observed when a D<sub>2</sub>R mutant lacking this sequence (D<sub>2</sub>R<sup>428–443</sup>) fused to Rluc was co-expressed with NCS-1-YFP (Figure S1C; top-left graph). In addition, a significant but partial modification of the D<sub>2</sub>R-Rluc/calneuron-1 BRET saturation curve was obtained with D<sub>2</sub>R<sup>428–443</sup>-Rluc (Figure S1C; top-right graph). A partial modification of the D<sub>2</sub>R-Rluc/calneuron-1 BRET saturation curve was also obtained with the short isoform of D<sub>2</sub>R fused to Rluc (D<sub>2S</sub>R-Rluc; which lacks an Arg-rich epitope in the middle of the 3IL of the long isoform) (Figure S1C; bottom-right graph). On the other hand no significant differences were observed between D<sub>2S</sub>R-Rluc/NCS-1 BRET saturation curves (Figure S1C; bottom-left graph). These results reinforce the assumption that the C-terminal domain of D<sub>2</sub>R is sufficient for NCS-1 binding and indicate that both the C-terminal domain and the 3IL of D<sub>2</sub>R are involved in calneuron-1 binding. The role of the D<sub>2</sub>R C-terminal domain in the interaction with both Ca<sup>2+</sup>-binding proteins was confirmed with surface plasmon resonance measurements using a peptide with the amino acid sequence of the C terminal domain of the D<sub>2</sub>R coupled to the biosensor (Figure S2; bottom graphs).

### Differential modulation by NCS-1 and calneuron-1 of allosteric interactions within A<sub>2A</sub>R-D<sub>2</sub>R heteromers

In HEK-293T cells expressing A<sub>2A</sub>R alone or A<sub>2A</sub>R and D<sub>2</sub>R, the A<sub>2A</sub>R agonist CGS 21680 (100 nM) induced ERK1/2 phosphorylation, which was completely blocked by the protein kinase A inhibitor H89 (Figure S3), indicating a G-protein-cAMP-PKA-dependent A<sub>2A</sub>R-mediated MAPK activation. In cells expressing A<sub>2A</sub>R and the D<sub>2</sub>R, CGS 21680 and the D<sub>2</sub>R agonist quinpirole (1 μM) induced a similar degree of ERK1/2 phosphorylation, in the presence or absence of ionomycin (Figure 4A; black bars). The absence of additive effect indicates the presence of moderate negative crosstalk, a negative allosteric interaction between both ligands within the A<sub>2A</sub>R-D<sub>2</sub>R heteromer. Similar effects were observed in cells expressing NCS-1, in the absence or in the presence of ionomycin, (Figure 4A; grey bars), as well as in cells expressing calneuron-1, but only in the absence of ionomycin (Figure 4A; left graph; white bars). In the presence of calneuron-1 and ionomycin, a strong negative crosstalk was observed, without increase of ERK1/2 phosphorylation over basal level and with significantly lower values upon co-administration of CGS 21680 plus quinpirole compared to CGS 21680 alone (Figure 4A; right graph; white bars). As negative

control, this effect was not observed when using the truncated mutant of calneuron-1, not able to bind to the A<sub>2A</sub>R or D<sub>2</sub>R (Figure S4A). These results suggest that, at high, but not low intracellular levels of Ca<sup>2+</sup>, calneuron-1 selectively facilitates a reciprocal negative allosteric interaction between CGS-21680 and quinpirole at the level of MAPK signaling in the A<sub>2A</sub>R-D<sub>2</sub>R heteromer.

In HEK-293T cells expressing A<sub>2A</sub>R and D<sub>2</sub>R receptors CGS 21680 (100 nM) increased cAMP accumulation and quinpirole (1 μM) decreased forskolin-induced cAMP accumulation in the absence or in the presence of ionomycin (Figure 4B; black bars). However, quinpirole did not counteract CGS 21680-induced cAMP accumulation (Figures 4B; black bars), indicating the existence of a strong negative allosteric modulation by which CGS 21680 significantly decreases the intrinsic efficacy of quinpirole as inhibitor of AC signaling. This modulation was also observed in cells expressing calneuron-1 in the absence of ionomycin (Figure 4B; left graph; white bars) and in cells expressing NCS-1, but in the presence of ionomycin (Figure 4B; right graph; white bars). In contrast, quinpirole was able to reduce cAMP accumulation induced by CGS 21680 in cells expressing calneuron-1 in the presence of ionomycin (Figure 4B; right graph; white bars) and in cells expressing NCS-1 but in the absence of ionomycin (Figure 4B; left graph; grey bars). As negative controls, the ability of quinpirole to counteract cAMP accumulation induced by CGS 21680 in the presence of ionomycin and calneuron-1 was not detected in cells expressing mutants of A<sub>2A</sub>R or D<sub>2</sub>R not able to bind calneuron-1 (Figure S4B; left graph). These results suggest binding of calneuron-1 to both receptors in the A<sub>2A</sub>R-D<sub>2</sub>R heteromer is necessary to exert its modulation. The ability of quinpirole to counteract cAMP accumulation induced by CGS 21680 in the presence of NCS-1 and in the absence of ionomycin was not observed in cells expressing A<sub>2A</sub>R and the D<sub>2</sub>R mutant not able to bind NCS-1 (Figure S4B; right graph). But, in contrast to calneuron-1, the effect was observed for heteromers constituted by wild-type D<sub>2</sub>R and the A<sub>2A</sub>R mutant not able to bind NCS-1 (Figure S7B; right graph), indicating that binding of NCS-1 to D<sub>2</sub>R, but not to the A<sub>2A</sub>R, in the heteromer is sufficient to exert its modulation.

### Ca<sup>2+</sup> levels determine the binding of NCS-1 and calneuron-1 to A<sub>2A</sub>R-D<sub>2</sub>R heteromers in striatal neurons

Proximity Ligation Assay (PLA) was used to confirm the expression of endogenous A<sub>2A</sub>R-D<sub>2</sub>R complexes in the primary cultures (Trifilieff et al., 2011). A<sub>2A</sub>R-D<sub>2</sub>R complexes could be observed as punctate red spots in neurons visualized by phase contrast and DAPI-stained nuclei (Figure 5A). The staining was observed in a high percentage of cells (>90 %), but not in negative controls in which one of the primary antibodies was omitted (Figure S5; control neurons). To evaluate the role of endogenous NCS-1 and calneuron-1 in the modulation of A<sub>2A</sub>R-D<sub>2</sub>R heteromer function, ERK1/2 phosphorylation was determined in neurons transfected with shRNA against NCS-1 or calneuron-1 mRNA. Knock down efficiency compared to control was verified by immunoblotting with specific antibodies against calneuron-1 or NCS1 and anti-tubulin antibodies as loading control (Figure S6). Transfection rate of calneuron-1 shRNA was analyzed by determination of GFP expression induced by the same plasmid under a different promoter (about 10,000 fluorescence units over basal background) and the expression of the NCS-1 shRNA was



determined by co-transfection with an empty GFP vector (about 8,000 fluorescence units over basal). Co-administration of CGS 21680 and quinpirole showed a partial or complete negative allosteric modulation between both ligands in the absence or in the presence of ionomycin, respectively (Figure 5B; black bars). This was equivalent to the negative allosteric modulation of A<sub>2A</sub>R and D<sub>2</sub>R ligands demonstrated in transfected HEK-293T cells. In fact, the complete negative allosteric modulation was observed in the presence of ionomycin (Figure 5B; right panel; black bars), which would be expected to depend on calneuron-1 (see Figure 4A; right panel; white bars). Indeed, tonic blockade of the negative crosstalk by endogenous calneuron-1 could be demonstrated, as silencing its expression led to a complete loss of the allosteric interaction in the presence of ionomycin (Figure 5B; right graph; white bars). Neither blockade of the expression of calneuron-1 in the absence of ionomycin (Figure 5B; left graph; white bars) nor blockade of the expression of NCS-1 in the presence or absence of ionomycin (Figure 5B; grey bars) significantly modified the effect of co-administration of CGS 21680 and quinpirole on ERK1/2 phosphorylation in striatal cells in culture.

CGS 21680 induced cAMP accumulation and quinpirole decreased forskolin-induced cAMP accumulation in the absence or in the presence of ionomycin (Figure 5C; black bars). Furthermore, quinpirole was able to reduce CGS 21680-induced cAMP in the absence or in the presence of ionomycin (Figure 5C; black bars). Thus, CGS 21680 could not significantly decrease the intrinsic efficacy of quinpirole as an inhibitor of AC signaling. Remarkably, the ability of CGS 21680 to fully counteract the inhibitory effect of quinpirole appeared with blockade of the expression of NCS-1 in the absence of ionomycin (Figure 5C; left graph; grey bars) and with blockade of calneuron-1 expression in the presence of ionomycin (Figure 5C; right graph; white bars). These results are in complete agreement with those obtained in HEK-293T cells. In striatal cells, however, intracellular Ca<sup>2+</sup> levels determine which neuronal Ca<sup>2+</sup> binding protein interacts with the A<sub>2A</sub>R-D<sub>2</sub>R heteromer.

PLA was also used to confirm the ability of Ca<sup>2+</sup> levels to determine which Ca<sup>2+</sup>-binding protein interacts with the A<sub>2A</sub>R-D<sub>2</sub>R heteromer in striatal neurons. Due to the lack of antibodies sufficiently specific for calneuron-1, only interactions with endogenous NCS-1 could be addressed. D<sub>2</sub>R-NCS-1 (Figure 6A, left panel), A<sub>2A</sub>R-NCS-1 (Figure 6A, middle) and A<sub>2A</sub>R-D<sub>2</sub>R (Figure 6A, left panel) complexes were readily observed in the absence of ionomycin as punctate red spots visualized by phase contrast and with DAPI-stained nuclei. As negative controls, red spots were not observed in the presence of only one of the primary antibodies (Figure S8; NCS-1 KD). The staining was observed in a high percentage of cells (Figure 6A; bar graphs). Although PLA can only assess close proximity between two proteins, the detection of A<sub>2A</sub>R-NCS-1, D<sub>2</sub>R-NCS-1 and A<sub>2A</sub>R-D<sub>2</sub>R complexes supports that A<sub>2A</sub>R-D<sub>2</sub>R-NCS-1 complexes are expressed in the same striatal neurons at low Ca<sup>2+</sup> levels. Importantly, in the presence of ionomycin, red spots were only observed for A<sub>2A</sub>R-D<sub>2</sub>R complexes (Figure 6A; right panel), but not for D<sub>2</sub>R-NCS-1 (Figure 6A; left panel) or A<sub>2A</sub>R-NCS-1 (Figure 6A; middle panel) complexes. To determine whether high Ca<sup>2+</sup> levels promote calneuron-1 binding to the heteromer, and circumventing the lack of specific calneuron-1 antibodies suitable for PLA, we transfected calneuron-1-YFP and used a specific anti-YFP antibody. A<sub>2A</sub>R-calneuron-1-YFP and D<sub>2</sub>R-calneuron-1-YFP complexes could be readily observed by PLA in the presence but not in the absence of ionomycin

(Figure 6B). The staining was observed in a high percentage of cells only in the presence of ionomycin (Figures 6B; bar graphs). These results from PLA experiments are in complete agreement with low and high  $\text{Ca}^{2+}$  levels promoting NCS-1 and calneuron-1 binding to the  $\text{A}_{2\text{A}}\text{R}$ - $\text{D}_2\text{R}$  heteromer, respectively.

## DISCUSSION

The present results provide new general findings about the physiological modulation of GPCR heteromer function: first, they demonstrate that in neurons, different  $\text{Ca}^{+2}$  levels can determine the binding of different neuronal  $\text{Ca}^{+2}$ -binding-proteins to a GPCR heteromer; second, they demonstrate that the binding of different neuronal  $\text{Ca}^{+2}$ -binding proteins can promote or disrupt different allosteric modulations in a GPCR heteromer; and third, we show that these differential effects allow a selective modulation of specific GPCR heteromer-dependent signaling pathways.

The strikingly similar results of signaling experiments obtained from HEK-293T transfected cells and striatal cells in culture allows us to formulate an heuristic model, which encapsulates previous biochemical findings in the frame of the heteromer, such as: a canonical antagonistic  $\text{G}_s$ - $\text{G}_i$  interaction at the level of AC signaling between  $\text{A}_{2\text{A}}\text{R}$  and  $\text{D}_2\text{R}$  (Kull et al., 1999; Hillion et al., 2002; Kudlacek et al., 2003), a predominant G-protein-cAMP-PKA-dependent  $\text{A}_{2\text{A}}\text{R}$ -mediated MAPK activation (present results and Klinger et al., 2002; Canals et al., 2005) and a predominant G-protein independent MAPK activation mediated by  $\text{D}_2\text{R}$  when co-expressed with  $\text{A}_{2\text{A}}\text{R}$  (Huang et al., 2013). Finally, the model assumes the recently proposed tetrameric structure of receptor heteromers (Ferré et al., 2014; Guitart et al., 2014).

The model proposes two independent  $\text{A}_{2\text{A}}\text{R}$ -mediated inhibitions of two different  $\text{D}_2\text{R}$ -mediated signaling pathways: MAPK activation (G protein-independent) and AC inhibition (G-protein-dependent) (Figure 7). Accumulation of cAMP only occurs upon single or predominant activation of the  $\text{A}_{2\text{A}}\text{R}$  in the heteromer, i.e., with low concentrations of dopamine. Under these conditions, the well-known  $\text{A}_{2\text{A}}\text{R}$ -agonist mediated decrease of the affinity of  $\text{D}_2\text{R}$  agonists counteracts any  $\text{D}_2\text{R}$ -mediated signaling through the heteromer, including AC inhibition. Co-activation with high concentrations of dopamine or  $\text{D}_2\text{R}$  specific agonists should surmount the decrease in affinity induced by  $\text{A}_{2\text{A}}\text{R}$  agonists and allow  $\text{D}_2\text{R}$  agonists to inhibit AC activity. However, in HEK-293T transfected cells in the absence of  $\text{Ca}^{+2}$ -binding proteins, co-activation of both receptors produced similar cAMP levels than those promoted by the  $\text{A}_{2\text{A}}\text{R}$  agonist, indicating that it is also possible to observe an  $\text{A}_{2\text{A}}\text{R}$  agonist-induced allosteric modulation of the intrinsic efficacy of  $\text{D}_2\text{R}$  agonists (Figure 7, left panel). This modulation, nevertheless, is disrupted with low and high  $\text{Ca}^{+2}$  levels in the presence of NCS-1 and calneuron-1, respectively, and the modulation is absent in striatal neurons in culture with low or high intracellular  $\text{Ca}^{+2}$  levels (because of the endogenous binding of NCS-1 or calneuron-1, respectively). Low levels of cAMP are then produced upon co-activation of the heteromer under these conditions (Figure 7, middle and right panels). Low  $\text{Ca}^{+2}$  levels (with NCS-1 binding), but not high  $\text{Ca}^{+2}$  levels (with calneuron-1 binding) disrupt the  $\text{A}_{2\text{A}}\text{R}$ -mediated negative crosstalk of the  $\text{D}_2\text{R}$ -mediated MAPK activation (Figure 7, middle and right panels). In summary, the allosteric modulation



mediated by neuronal  $\text{Ca}^{+2}$ -binding proteins determines that in the  $\text{A}_{2\text{A}}\text{R}$ - $\text{D}_2\text{R}$  heteromer a preferential activation of  $\text{A}_{2\text{A}}\text{R}$  leads to both cAMP accumulation and MAPK signaling; upon co-activation of  $\text{A}_{2\text{A}}\text{R}$  and  $\text{D}_2\text{R}$ , the presence of low intracellular  $\text{Ca}^{+2}$  levels leads only to MAPK signaling and, at high  $\text{Ca}^{+2}$  levels, co-activation leads to a very diminished  $\text{A}_{2\text{A}}\text{R}$ - $\text{D}_2\text{R}$  heteromer-mediated signaling response.

Previous reports have shown that, depending on the neuronal function under study, co-activation of  $\text{A}_{2\text{A}}\text{R}$  and  $\text{D}_2\text{R}$  leads to significant inhibition of  $\text{A}_{2\text{A}}\text{R}$  or  $\text{D}_2\text{R}$ -mediated response, indicating the existence of reciprocal interactions between both receptors that modulate different functional responses. In the striatum, stimulation of  $\text{A}_{2\text{A}}\text{R}$  counteracts a  $\text{D}_2\text{R}$  agonist-induced inhibitory modulation of NMDA receptor-mediated effects (Azdad et al., 2009; Higley and Sabatini, 2010), which are dependent on an increase in intracellular  $\text{Ca}^{+2}$  levels. On the other hand, the ability of  $\text{A}_{2\text{A}}\text{R}$  to activate AC seems to be normally restrained by a strong tonic inhibitory effect of endogenous dopamine on striatal  $\text{D}_2\text{R}$ , which efficiently inhibits  $\text{A}_{2\text{A}}\text{R}$ -mediated AC activation (Svenningsson et al., 1999). To explain the co-existence of these simultaneous reciprocal antagonistic interactions between striatal  $\text{A}_{2\text{A}}\text{R}$  and  $\text{D}_2\text{R}$ , we previously postulated their mediation by two different populations of  $\text{A}_{2\text{A}}\text{R}$ , forming and not forming heteromers with  $\text{D}_2\text{R}$  (Ferré et al., 2011). The present results allow understanding the co-existence of these interactions considering only one predominant population of  $\text{A}_{2\text{A}}\text{R}$ , which forms heteromers with  $\text{D}_2\text{R}$ . This could account for different G protein-dependent or independent functional responses, which could be differentially modulated by intracellular  $\text{Ca}^{+2}$  levels. Apart from adenosine and dopamine, the  $\text{Ca}^{+2}$ -dependent modulation of  $\text{A}_{2\text{A}}\text{R}$ - $\text{D}_2\text{R}$  heteromer function allows further integration of other neurotransmitter systems such as glutamate (through NMDA receptor activation) and acetylcholine (through Gq-coupled muscarinic receptors) (Tozzi et al., 2011).

## SIGNIFICANCE

The present study demonstrates that GPCR heteromers are cellular devices that provide a very elaborate integration and modulation of signals from different neurotransmitters that ultimately depends on physiological factors such as intracellular  $\text{Ca}^{+2}$  levels.  $\text{Ca}^{+2}$  levels, through different  $\text{Ca}^{+2}$ -binding proteins, determine functional selectivity within the  $\text{A}_{2\text{A}}\text{R}$ - $\text{D}_2\text{R}$  heteromer, which is an important target for the treatment of Parkinson's disease and other neuropsychiatric disorders.

## EXPERIMENTAL PROCEDURES

### Vectors, fusion proteins and mutant proteins

The cDNA constructs encoding human  $\text{A}_{2\text{A}}\text{R}$ ,  $\text{D}_2\text{R}$ ,  $\text{D}_{2\text{s}}\text{R}$  or calmodulin in pcDNA3 vectors were subcloned in pEYFP-N1 (enhanced yellow variant of GFP; Clontech, Heidelberg, Germany), pRluc-N1 (PerkinElmer, Wellesley, MA) or pGFP-2-N1 (Biosignal) vectors as previously described (Navarro et al., 2009) to generate  $\text{A}_{2\text{A}}\text{R}$ -YFP,  $\text{A}_{2\text{A}}\text{R}$ -Rluc,  $\text{A}_{2\text{A}}\text{R}$ -GFP<sup>2</sup>,  $\text{D}_2\text{R}$ -YFP,  $\text{D}_2\text{R}$ -Rluc,  $\text{D}_{2\text{s}}\text{R}$ -Rluc or  $\text{D}_2\text{R}$ -GFP<sup>2</sup> fusion proteins. cDNA constructs encoding NCS-1 or caldendrin in pcDNA3 vectors were subcloned in pEYFP-N1 or in pGFP-2-N1 vectors as previously described (Navarro et al., 2012) to generate NCS-1-YFP, caldendrin-YFP or NCS-1-GFP<sup>2</sup> fusion proteins. The cDNA for calneuron, cloned into

pcDNA3.1, was amplified without its stop codons using sense and antisense primers harboring unique BamHI and HindII sites to clone calneuron-1 in pcDNA3.1RLuc vector or HindIII and BamHI to clone in pEYFP-N1 vector or to clone in pGFP-2-N1 vector. The amplified fragments were subcloned to be in-frame with restriction sites of the corresponding vectors to give the plasmids that express calneuron-1-RLuc, calneuron-1-YFP or calneuron-1-GFP<sup>2</sup>. The sequence <sup>199</sup>RIFLAARRQ<sup>207</sup> in the cytoplasm at the end of TM5 of human A<sub>2A</sub>R was mutated to <sup>199</sup>RIFLAAAQ<sup>207</sup> to obtain the A<sub>2A</sub>R<sup>A205-A206</sup> as previously described (Navarro et al., 2010). The D<sub>2</sub>R<sup>428-443</sup> was generated by deletion of the last 16 amino acids from the D<sub>2</sub>R and subcloned harboring EcoRI and KpnI restriction sites in pRLuc-N1. Calneuron-1 construct truncated in the C-terminus (calneuron-1 CT) and N-terminal myristoylation-deficient NCS-1 mutant in which YFP is fused to the N-terminus of NCS-1 were obtained as described elsewhere (Hradsky et al., 2011). Fusion proteins corresponding to mutant proteins were obtained following the methodology above described.

### Primary cultures of rat striatal neurons, cell lines and transfection

Primary cultures of striatal neurons were obtained from fetal Sprague Dawley rats of 19 days. Striatal cells were isolated as described in (Hradsky et al., 2013) and plated at confluence of 40.000 cells/0,32 cm<sup>2</sup>. Cells were grown in Neurobasal medium supplemented with 2 mM L-glutamine, 100 U/ml penicillin/streptomycin, and 2% (v/v) B27 supplement (Gibco) in a 96 well plate for 12 days. HEK-293T cells were grown in Dulbecco's modified Eagle's medium (DMEM) supplemented with 2 mM L-glutamine, 100 U/ml penicillin/streptomycin, and 5% (v/v) heat inactivated Fetal Bovine Serum (FBS) (Invitrogen, Paisley, Scotland, UK). Primary cultures or HEK-293T cells were cultured in the corresponding growth medium in the absence of ionomycin or in the presence of 1 μM of ionomycin. Striatal neurons and HEK-293T cells were transfected with the plasmids encoding receptors and/or calcium binding proteins by the PEI (PolyEthylenImine, Sigma, Steinheim, Germany) method as previously described (Carriba et al., 2008).

### Resonance Energy Transfer experiments

Described in detailed elsewhere (Carriba et al., 2008; Navarro et al., 2009, 2010, 2012), figure legends and in supplementary material.

### Surface plasmon resonance (SPR)

Surface plasmon resonance measurements were performed on a Biacore X100 system (GE Healthcare) to determine the calcium binding proteins interaction with GST coupled to A<sub>2A</sub>R third intracellular loop (GST-A<sub>2A</sub>R-IL3) or with D<sub>2</sub>R C-terminal domain peptide (P14416, pos. 432–443, peptide purchased from PSL GmbH, Germany) coupled to a CM5 sensor chip according to the manufacturers protocol (D<sub>2</sub>R-Cterm). Described in detailed elsewhere (Catimel et al., 1997; Mikhaylova et al., 2009) and figure legend (Figure S2).

### Immunocytochemistry

Immunocytochemistry assays were performed as previously described (Navarro *et al*, 2009) using the primary antibodies mouse anti-A<sub>2A</sub>R (1/200; Millipore) or mouse anti-D<sub>2</sub>R (1/200; Santa Cruz) and stained with the secondary antibodies Cy3 anti-mouse (1/200; Jackson

ImmunoResearch). NCS-1, calneuron-1 or caldendrin fused to YFP protein were detected by its fluorescence properties. Samples were observed in a Leica SP2 confocal microscope (Leica Microsystems).

### **Knock down endogenous calneuron-1 or NCS-1 in primary cultures of rat striatal neurons**

Primary striatal neurons growing in 6 well dishes were transfected with the PEI method to knock down the NCS-1 or calneuron-1 expression using calneuron-1 shRNAII (1xconstruct #2; genecopoeia) with psi-HIV-H1 backbone and eGFP as a marker or pSuper-NCS-1 vector. Cells were incubated for 6–8 h with the cDNA and the PEI (5.47 mM in nitrogen residues) and 150 mM in NaCl in serum-starved medium. After 6–8 hours medium was replaced with complete culture medium. 48 h post-transfection the GFP<sup>2</sup> fluorescence signal was detected to test the transfection efficiency. Striatal neurons were then detached and calneuron-1 and NCS-1 expression was detected by Western blotting (see results).

### **Cell signaling**

The cAMP concentration was determined by Homogeneous Time-Resolved Fluorescence (HTRF) energy transfer assay. Lance Ultra cAMP kit (PerkinElmer, Waltham, MA, USA), based on a europium chelate-labelled cAMP tracer, was used. Cells (4000 cells/well for transfected HEK-293T cells or 6000 cells/well for primary cultures of striatal neurons) were stimulated with agonists for 15 min in serum-starved DMEM medium supplemented with 50  $\mu$ M zardeverine, 5 mM HEPES and 0,1% BSA with or without 1  $\mu$ M ionomycin, before adding 0.5  $\mu$ M forskolin or vehicle, and incubating for an additional 15 min-period. Fluorescence at 665 nm was analyzed on a PHERAstar Flagship microplate reader equipped with an HTRF optical module (BMG Labtechnologies, Offenburg, Germany). ERK 1/2 phosphorylation was determined using the AlphaScreen SureFire kit (Perkin Elmer) following the instructions of the supplier and using an EnSpire Multimode Plate Reader (PerkinElmer, Waltham, MA, USA). Cells (30.000 cells/well for transfected HEK-293T cells or 40.000 cells/well for primary cultures) were seeded in white ProxiPlate 384-well microplates, pre-treated at 25°C for 20 min with vehicle or antagonists in serum-starved DMEM medium supplemented or nor with 1  $\mu$ M ionomycin and stimulated for an additional 7 min with the indicated agonists.

### **Proximity Ligation Assays (PLA)**

Heteromers were detected using the Duolink II in situ PLA detection Kit (OLink; Bioscience, Uppsala, Sweden) following the instructions of the supplier. Primary cultures of striatal neurons were grown on glass coverslips and were fixed in 4% paraformaldehyde for 15 min, washed with PBS containing 20 mM glycine to quench the aldehyde groups, permeabilized with the same buffer containing 0.05% Triton X-100 for 5 min and successively washed with PBS. After 1 h incubation at 37°C with the blocking solution in a pre-heated humidity chamber, primary cultures were incubated overnight in the antibody diluent medium with a mixture of equal amounts of mouse monoclonal anti-A<sub>2A</sub>R antibody (1:200, Millipore) and the goat polyclonal anti-D<sub>2</sub>R antibody (1:200, Santa Cruz) to detect A<sub>2A</sub>R-D<sub>2</sub>R heteromers, with the goat polyclonal anti-D<sub>2</sub>R antibody and a polyclonal rabbit anti-NCS-1 antibody (1:200, FL190, Santa Cruz) to detect D<sub>2</sub>R-NCS-1 complexes, with mouse monoclonal anti-A<sub>2A</sub>R antibody and the rabbit polyclonal anti-NCS-1 antibody to

detect A<sub>2A</sub>R-NCS-1 complexes, with goat polyclonal anti-D<sub>2</sub>R antibody and rabbit anti-GFP antibody (1/200, Molecular Probes) to detect D<sub>2</sub>R-calneuron-1-YFP complexes or mouse monoclonal anti-A<sub>2A</sub>R antibody and rabbit anti-GFP antibody to detect A<sub>2A</sub>R-calneuron-1-YFP complexes. Cells were processed using the PLA probes detecting mouse and goat antibodies (Duolink II PLA probe anti-Mouse plus and Duolink II PLA probe anti-Goat minus) or goat and rabbit antibodies (Duolink II PLA probe anti-Goat plus and Duolink II PLA probe anti-Rabbit minus) or mouse and rabbit antibodies (Duolink II PLA probe anti-Mouse plus and Duolink II PLA probe anti-Rabbit minus) diluted in the antibody diluent to a concentration of 1:5. Ligation and amplification were done as indicated by the supplier and cells were mounted using the mounting medium with Hoechst (1/200; Sigma). Samples were observed in a Leica SP2 confocal microscope (Leica Microsystems, Mannheim, Germany) equipped with an apochromatic 63X oil-immersion objective (N.A. 1.4), and a 405 nm and a 561 nm laser lines. For each field of view a stack of two channels (one per staining) and 4 to 8 Z stacks with a step size of 1 µm were acquired. A quantification of cells containing one or more red spots versus total cells (blue nucleus) and, in cells containing spots, the ratio r (number of red spots/ cell), were determined considering a total 25–40 cells from 10–20 different fields using the ImageJ confocal program. Nuclei and red spots were counted on the maximum projections of each image stack. One-way ANOVA followed by Dunet's *post hoc* multiple comparison test was used to compare the values (% of positive cells or r –spots/cell-) obtained for each pair of receptors.

## Supplementary Material

Refer to Web version on PubMed Central for supplementary material.

## Acknowledgements

Work supported by the intramural funds of the National Institute on Drug Addiction, from the Spanish “Ministerio de Ciencia y Tecnología” (SAF2011-23813), the Government of Catalonia (2009-SGR-12), CIBERNED (CB06/05/0064), German Research Foundation (SFB779/TPB8, DFG Kr1879/3-1), the Leibniz Foundation (Pakt f. Forschung), European Molecular Biology Organization Long-Term Fellowship (to M.M., EMBO ALTF 884-2011), the European Commission (EMBOCOFUND2010, GA-2010-267146), Marie Curie Actions (Intra-European Fellowship) and ‘Ramón y Cajal’ Fellowship (to P.J.M.).

## References

- Azdad K, Gall D, Woods AS, Ledent C, Ferré S, and Schiffmann SN (2009). Dopamine D2 and adenosine A2A receptors regulate NMDA-mediated excitation in accumbens neurons through A2A-D2 receptor heteromerization. *Neuropsychopharmacology* 34, 972–986. [PubMed: 18800071]
- Canals M, Angulo E, Casadó V, Canela EI, Mallol J, Viñals F, Staines W, Tinner B, Hillion J, Agnati L, et al. (2005) Molecular mechanisms involved in the adenosine A1 and A2A receptor-induced neuronal differentiation in neuroblastoma cells and striatal primary cultures. *J. Neurochem* 2, 337–348.
- Carriba P, Navarro G, Ciruela F, Ferré S, Casadó V, Agnati L, Cortés A, Mallol J, Fuxe K, Canela EI, et al. (2008). Detection of heteromerization of more than two proteins by sequential BRET-FRET. *Nat. Methods* 5, 727–733. [PubMed: 18587404]
- Catimel B, Nerrie M, Lee FT, Scott AM, Ritter G, Welt S, Old LJ, Burgess AW, and Nice EC (1997). Kinetic analysis of the interaction between the monoclonal antibody A33 and its colonic epithelial antigen by the use of an optical biosensor. A comparison of immobilisation strategies. *J. Chromatogr. A* 776, 15–30. [PubMed: 9286074]

- Ferré S, von Euler G, Johansson B, Fredholm BB, and Fuxe K (1991). Stimulation of high-affinity adenosine A2 receptors decreases the affinity of dopamine D2 receptors in rat striatal membranes. *Proc. Natl. Acad. Sci. USA* 88, 7238–7241. [PubMed: 1678519]
- Ferré S, Baler R, Bouvier M, Caron MG, Devi LA, Durroux T, Fuxe K, George SR, Javitch JA, Lohse MJ, et al. (2009). Building a new conceptual framework for receptor heteromers. *Nat. Chem. Biol* 5, 131–134. [PubMed: 19219011]
- Ferré S, Woods AS, Navarro G, Aymerich M, Lluís C, and Franco R (2010). Calcium-mediated modulation of the quaternary structure and function of adenosine A2A-dopamine D2 receptor heteromers. *Curr. Opin. Pharmacol* 10, 67–72. [PubMed: 19896897]
- Ferré S, Quiroz C, Orru M, Guitart X, Navarro G, Cortés A, Casadó V, Canela EI, Lluís C, and Franco R (2011). Adenosine A(2A) Receptors and A(2A) Receptor heteromers as key players in striatal function. *Front. Neuroanat* 5, 36. [PubMed: 21731559]
- Ferré S, Casadó V, Devi LA, Filizola M, Jockers R, Lohse MJ, Milligan G, Pin JP, and Guitart X (2014). G protein-coupled receptor oligomerization revisited: functional and pharmacological perspectives. *Pharmacol. Rev* 66, 413–434. [PubMed: 24515647]
- Guitart X, Navarro G, Moreno E, Yano H, Cai NS, Sanchez M, Kumar-Barodia S, Naidu Y, Mallol J, Cortes A, et al. (2014) Functional selectivity of allosteric interactions within GPCR oligomers: the dopamine D<sub>1</sub>-D<sub>3</sub> receptor heterotetramer. *Mol. Pharmacol* (in press).
- Hillion J, Canals M, Torvinen M, Casado V, Scott R, Terasmaa A, Hansson A, Watson S, Olah ME, Mallol J, et al. (2002). Coaggregation, cointernalization, and codesensitization of adenosine A2A receptors and dopamine D2 receptors. *J. Biol. Chem* 277, 18091–18097. [PubMed: 11872740]
- Higley MJ, and Sabatini BL (2010) Competitive regulation of synaptic Ca<sup>2+</sup> influx by D2 dopamine and A2A adenosine receptors. *Nat Neurosci* 13, 958–66. [PubMed: 20601948]
- Hradsky J, Raghuram V, Reddy PP, Navarro G, Hupe M, Casado V, McCormick PJ, Sharma Y, Kreutz MR, and Mikhaylova M (2011). Post-translational membrane insertion of tail-anchored transmembrane EF-hand Ca<sup>2+</sup> sensor calneurons requires the TRC40/Asna1 protein chaperone. *J. Biol. Chem* 286, 36762–36776. [PubMed: 21878631]
- Hradsky J, Mikhaylova M, Karpova A, Kreutz MR, and Zuschratter W (2013). Super-resolution microscopy of the neuronal calcium-binding proteins Calneuron-1 and Caldendrin. *Methods Mol. Biol* 963, 147–169. [PubMed: 23296610]
- Huang L, Wu DD, Zhang L, and Feng LY (2013). Modulation of A2A receptor antagonist on D2 receptor internalization and ERK phosphorylation. *Acta Pharmacol. Sin* 34, 1292–1300. [PubMed: 23933651]
- Kabbani N, Negyessy L, Lin R, Goldman-Rakic P, and Levenson R (2002). Interaction with neuronal calcium sensor NCS-1 mediates desensitization of the D2 dopamine receptor. *J. Neurosci* 22, 8476–8486. [PubMed: 12351722]
- Klinger M, Kudlacek O, Seidel MG, Freissmuth M, Sexl V (2002). MAP kinase stimulation by cAMP does not require RAP1 but SRC family kinases. *J. Biol. Chem* 277, 32490–32497. [PubMed: 12082090]
- Kull B, Ferré S, Arslan G, Svenningsson P, Fuxe K, Owman C, and Fredholm BB (1999). Reciprocal interactions between adenosine A2A and dopamine D2 receptors in Chinese hamster ovary cells co-transfected with the two receptors. *Biochem. Pharmacol* 58, 1035–1045. [PubMed: 10509756]
- Mikhaylova M, Reddy PP, Munsch T, Landgraf P, Suman SK, Smalla KH, Gundelfinger ED, Sharma Y, and Kreutz MR (2009) Calneurons provide a calcium threshold for trans-Golgi network to plasma membrane trafficking. *Proc. Natl. Acad. Sci. USA* 106, 9093–9098. [PubMed: 19458041]
- Mikhaylova M, Hradsky J, and Kreutz MR (2011). Between promiscuity and specificity: novel roles of EF-hand calcium sensors in neuronal Ca<sup>2+</sup> signalling. *J. Neurochem* 118, 695–713. [PubMed: 21722133]
- Navarro G, Aymerich MS, Marcellino D, Cortés A, Casadó V, Mallol J, Canela EI, Agnati L, Woods AS, Fuxe K, et al. (2009). Interactions between calmodulin, adenosine A2A, and dopamine D2 receptors. *J. Biol. Chem* 284, 28058–28068. [PubMed: 19632986]
- Navarro G, Ferré S, Cordomi A, Moreno E, Mallol J, Casadó V, Cortés A, Hoffmann H, Ortiz J, Canela EI, et al. (2010). Interactions between intracellular domains as key determinants of

the quaternary structure and function of receptor heteromers. *J. Biol. Chem* 285, 27346–27359. [PubMed: 20562103]

- Navarro G, Hradsky J, Lluís C, Casadó V, McCormick PJ, Kreutz MR, and Mikhaylova M (2012). NCS-1 associates with adenosine A(2A) receptors and modulates receptor function. *Front. Mol. Neurosci* 5, 53. [PubMed: 22529776]
- Saab BJ, Georgiou J, Nath A, Lee FJ, Wang M, Michalon A, Liu F, Mansuy IM, and Roder JC (2009). NCS-1 in the dentate gyrus promotes exploration, synaptic plasticity, and rapid acquisition of spatial memory. *Neuron* 63, 643–656. [PubMed: 19755107]
- Svenningsson P, Fourreau L, Bloch B, Fredholm BB, Gonon F, and Le Moine C (1999). Opposite tonic modulation of dopamine and adenosine on c-fos gene expression in striatopallidal neurons. *Neuroscience* 89, 827–837. [PubMed: 10199616]
- Tozzi A, de Iure A, Di Filippo M, Tantucci M, Costa C, Borsini F, Ghiglieri V, Giampà C, Fusco FR, Picconi B, et al. (2011). The distinct role of medium spiny neurons and cholinergic interneurons in the D<sub>2</sub>/A<sub>2A</sub> receptor interaction in the striatum: implications for Parkinson's disease. *J. Neurosci* 31, 1850–1862. [PubMed: 21289195]
- Trifilieff P, Rives ML, Urizar E, Piskowski RA, Vishwasrao HD, Castrillon J, Schmauss C, Slättman M, Gullberg M, and Javitch JA (2011). Detection of antigen interactions ex vivo by proximity ligation assay: endogenous dopamine D2 adenosine A2A receptor complexes in the striatum. *Biotechniques* 51, 111–118. [PubMed: 21806555]



**HIGHLIGHTS**

- $\text{Ca}^{2+}$  modulates adenosine  $\text{A}_{2\text{A}}$ -dopamine  $\text{D}_2$  receptor heteromer function in neurons
- $\text{Ca}^{2+}$  levels determine which neuronal  $\text{Ca}^{2+}$ -binding protein binds to the GPCR heteromer
- $\text{Ca}^{2+}$ -binding proteins promote functional selectivity within the GPCR heteromer

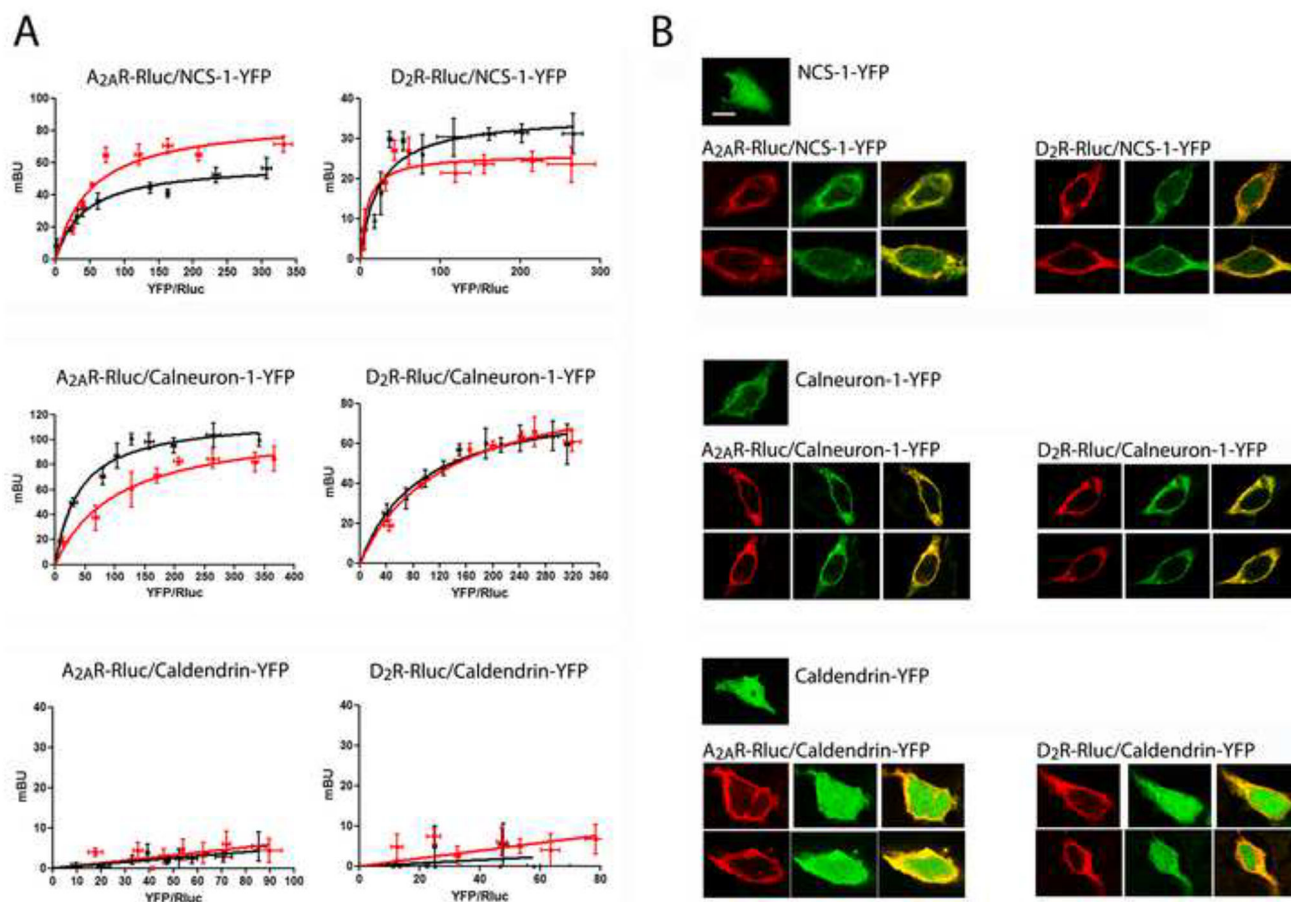


### Figure 1. NCS-1 and calneuron-1 but not caldendrin interact with A<sub>2A</sub>R and D<sub>2</sub>R

**A.** BRET saturation experiments in HEK-293T cells transfected with A<sub>2A</sub>R-Rluc cDNA (0.2 μg; left graphs) or D<sub>2</sub>R-Rluc cDNA (0.4 μg; right graphs) and increasing amounts of NCS-1-YFP cDNA (0.2 μg to 0.8 μg; top graphs), calneuron-1-YFP cDNA (0.4 μg to 1.2 μg; middle graphs) or caldendrin-YFP cDNA (0.2 μg to 1 μg; bottom graphs), in the absence (black curves) or in the presence (red curves) of 1 μM ionomycin. The relative amount of BRET is given as a function of 1000 × the ratio between the fluorescence of the acceptor (YFP) and the luciferase activity of the donor (Rluc). BRET is expressed as mili BRET units (mBU) and is given as means ± S.E.M. of 5 to 7 different experiments grouped as a function of the amount of BRET acceptor. **B.** Confocal microscopy images of HEK-293T cells transfected with NCS-1-YFP cDNA (0.5 μg; top panels), calneuron-1-YFP cDNA (0.7 μg; middle panels) or caldendrin-YFP cDNA (0.5 μg; bottom panels), co-transfected or not with A<sub>2A</sub>R-Rluc cDNA (0.4 μg; left panels) or D<sub>2</sub>R-Rluc cDNA (0.6 μg; right panels). Receptors were identified by immunocytochemistry (red) and proteins fused to YFP were identified by its own fluorescence (green). Co-localization is shown in yellow in merge figures. Scale bar: 10 μm.

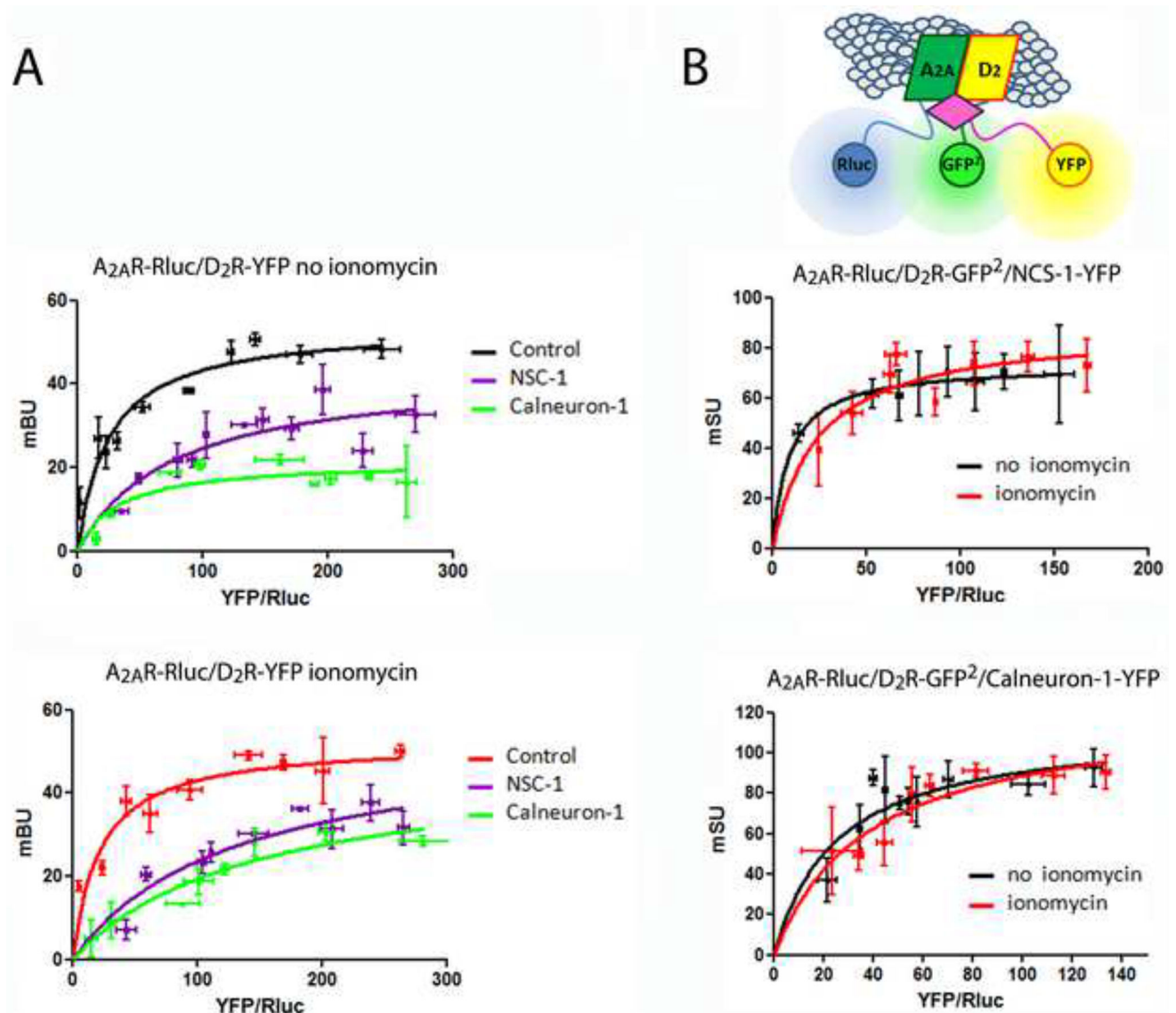


**Figure 2. NCS-1 and calneuron-1 interact with A<sub>2</sub>AR-D<sub>2</sub>R heteromers**

**A.** BRET saturation experiments in HEK-293T cells transfected with A<sub>2</sub>AR-Rluc cDNA (0.2 μg) and increasing amounts of D<sub>2</sub>R-YFP cDNA (0.1 μg to 1 μg) with or without NCS-1 cDNA (0.7 μg) or calneuron-1 cDNA (1), in the absence (top graph) or in the presence (bottom graph) of 1 μM ionomycin. **B.** Sequential Resonance Energy Transfer (SRET) SRET saturation experiments in HEK-293T cells transfected with A<sub>2</sub>AR-Rluc cDNA (0.3 μg), D<sub>2</sub>R-GFP<sup>2</sup> cDNA (0.4 μg) and increasing amounts of NCS-1-YFP cDNA (0.3 μg to 0.8 μg; top graph) or calneuron-1-YFP cDNA (0.5 μg to 1.5 μg; bottom graph) in the absence (black curves) or presence (red curves) of 1 μM ionomycin. Scheme shows SRET with the sequential BRET (Rluc as donor and GFP<sup>2</sup> as acceptor) and FRET (GFP<sup>2</sup> as donor and YFP as acceptor) processes. BRET or SRET are expressed as miliBRET or miliSRET units (mBU, mSU), respectively, and given as a function of 1000 × the ratio between the fluorescence of the acceptor (YFP) and the luciferase activity of the donor (Rluc). Values are means ± S.E.M. of 6 to 8 different experiments.

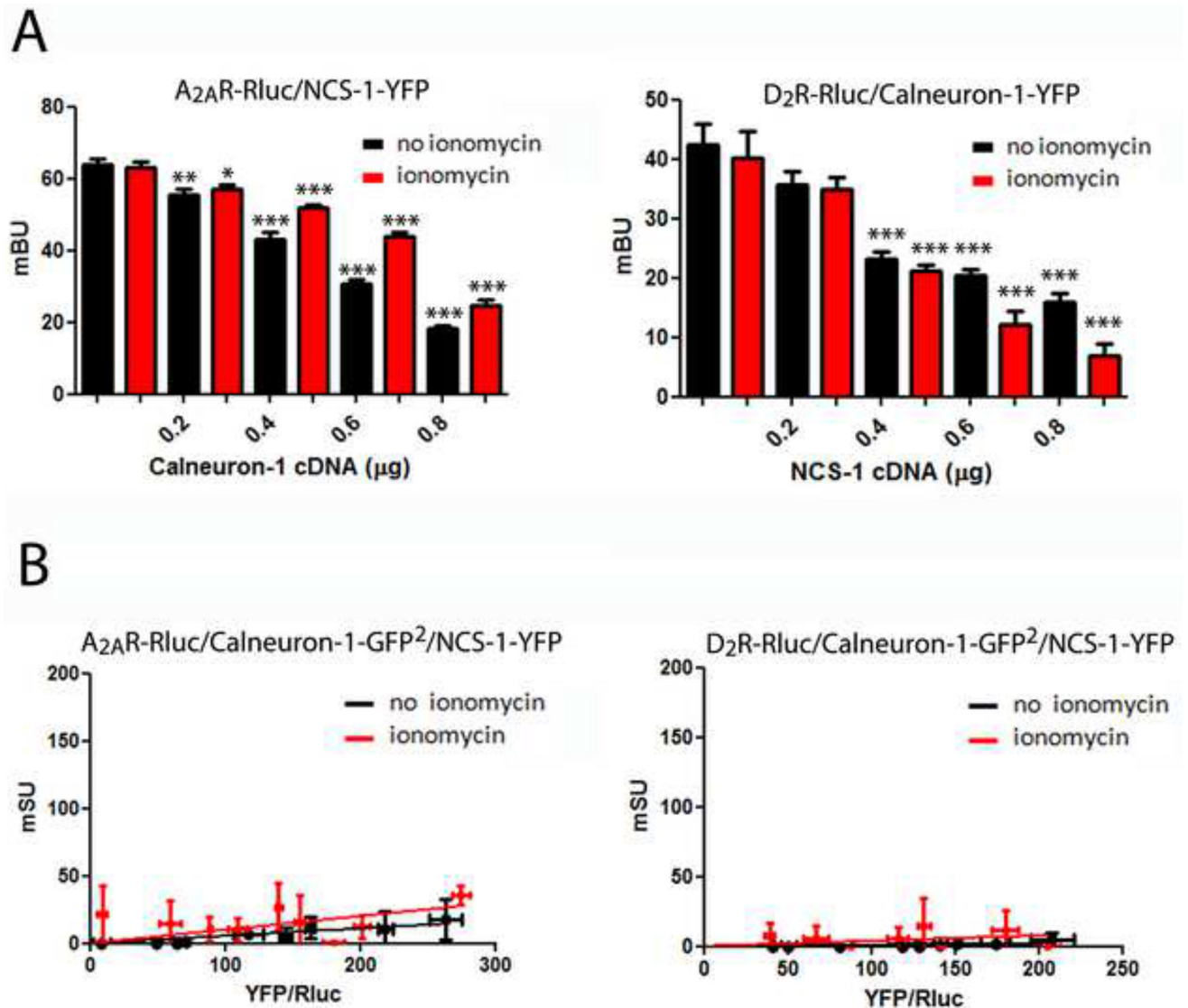


**Figure 3. NCS-1 and calneuron-1 compete for binding to A<sub>2</sub>A R and D<sub>2</sub> R**

**A.** BRET competition experiments in HEK-293T cells transfected with A<sub>2</sub>A-Rluc cDNA (0.2 μg) and NCS-1-YFP cDNA (0.7 μg) with increasing amounts of calneuron-1 cDNA (0.2 μg to 0.8 μg; left graph) or with D<sub>2</sub>R-Rluc cDNA (0.3 μg) and calneuron-1-YFP cDNA (1 μg; right graph) with increasing amounts of NCS-1 cDNA (0.2 μg to 0.8 μg, right graph) in the absence (black bars) or presence (red bars) of 1 μM ionomycin. BRET, expressed as miliBRET units (mBU), is given as means ± S.E.M. of 6 to 8 different experiments. One-way ANOVA followed by *post hoc* Dunnett's multiple comparisons: \*p < 0.05, \*\*p < 0.01 and \*\*\*p < 0.001 versus BRET in the absence of NCS-1 or calneuron-1. **B.** SRET in HEK-293T cells transfected A<sub>2</sub>A-Rluc cDNA (0.2 μg; left graphs) or D<sub>2</sub>R-Rluc cDNA (0.3 μg; right graph), and calneuron-1-GFP<sup>2</sup> cDNA (0.4 μg) and increasing amounts of NCS-1-YFP cDNA (0.2 μg to 0.8 μg) in the absence (black lines) or presence (red lines) of 1 μM ionomycin. The relative amount of SRET, expressed as miliSRET units (mSU), is given as a function of 1000 × the ratio between the fluorescence of the acceptor (YFP) and

the luciferase activity of the donor (Rluc). Values are means  $\pm$  S.E.M. of 4 to 6 different experiments.



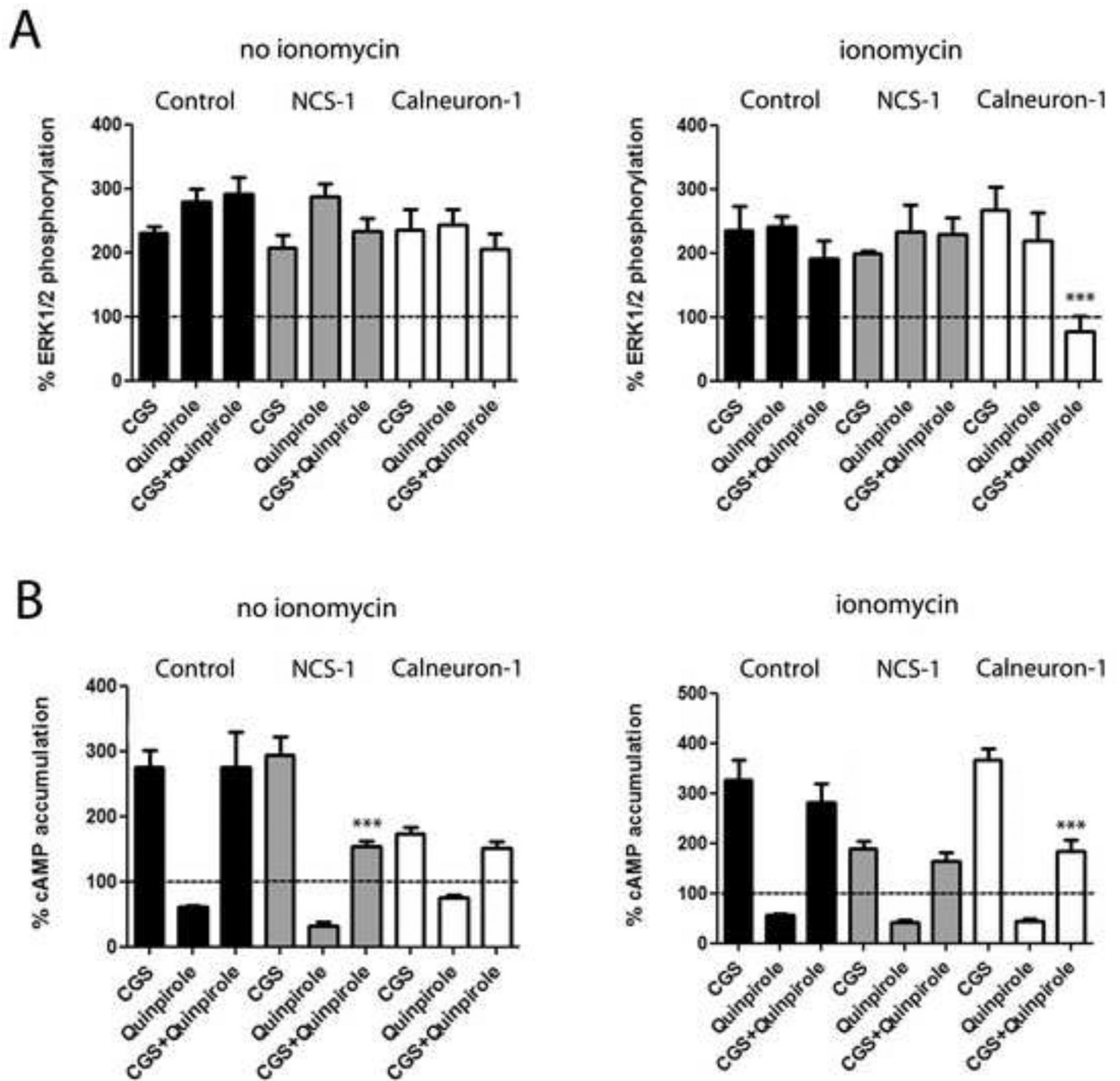


**Figure 4. Modulation by NCS-1 and calneuron-1 of  $A_2A$ R- $D_2$ R heteromer signaling in transfected cells**

**A.** ERK1/2 phosphorylation in HEK-293T cells transfected with  $A_2A$ R-Rluc cDNA (0.3  $\mu$ g) and  $D_2$ R-YFP cDNA (0.5  $\mu$ g) alone (black bars) or also transfected with NCS-1 cDNA (0.4  $\mu$ g cDNA; grey bars) or calneuron-1 cDNA (0.6  $\mu$ g; white bars) after administration of the  $A_2A$ R agonist CGS 21680 (CGS, 100 nM), the  $D_2$ R agonist quinpirole (1  $\mu$ M) or both, in the absence or presence of ionomycin (left and right graphs, respectively). ERK1/2 phosphorylation levels are expressed as a percentage over basal. **B.** Levels of cAMP in HEK-293T cells transfected with  $A_2A$ R-Rluc cDNA (0.3  $\mu$ g) and  $D_2$ R-YFP cDNA (0.5  $\mu$ g) alone (black bars) or also transfected with NCS-1 cDNA (0.4  $\mu$ g cDNA; grey bars) or



calneuron-1 cDNA (0.6  $\mu$ g; white bars) after administration of the A<sub>2A</sub>R agonist CGS 21680 (CGS, 100 nM), the D<sub>2</sub>R agonist quinpirole (1  $\mu$ M) or both, in the absence or presence of ionomycin (left and right graphs, respectively). Levels of cAMP after CGS alone or after CGS plus quinpirole are expressed as a percentage over basal; cAMP after quinpirole alone are expressed as percentage of decreases with respect to cAMP induced by forskolin (0.5  $\mu$ M); basal and forskolin-induced cAMP were given as 100% and represented by a dotted line. were determined in the absence (a and c) or presence (b and d) of 1  $\mu$ M ionomycin. Values are mean  $\pm$  S.E.M. of 4 to 6 different experiments. One-way ANOVA followed by *post hoc* Dunnett's multiple comparisons: \*\*\*p < 0.001 versus CGS 21680 treatment.

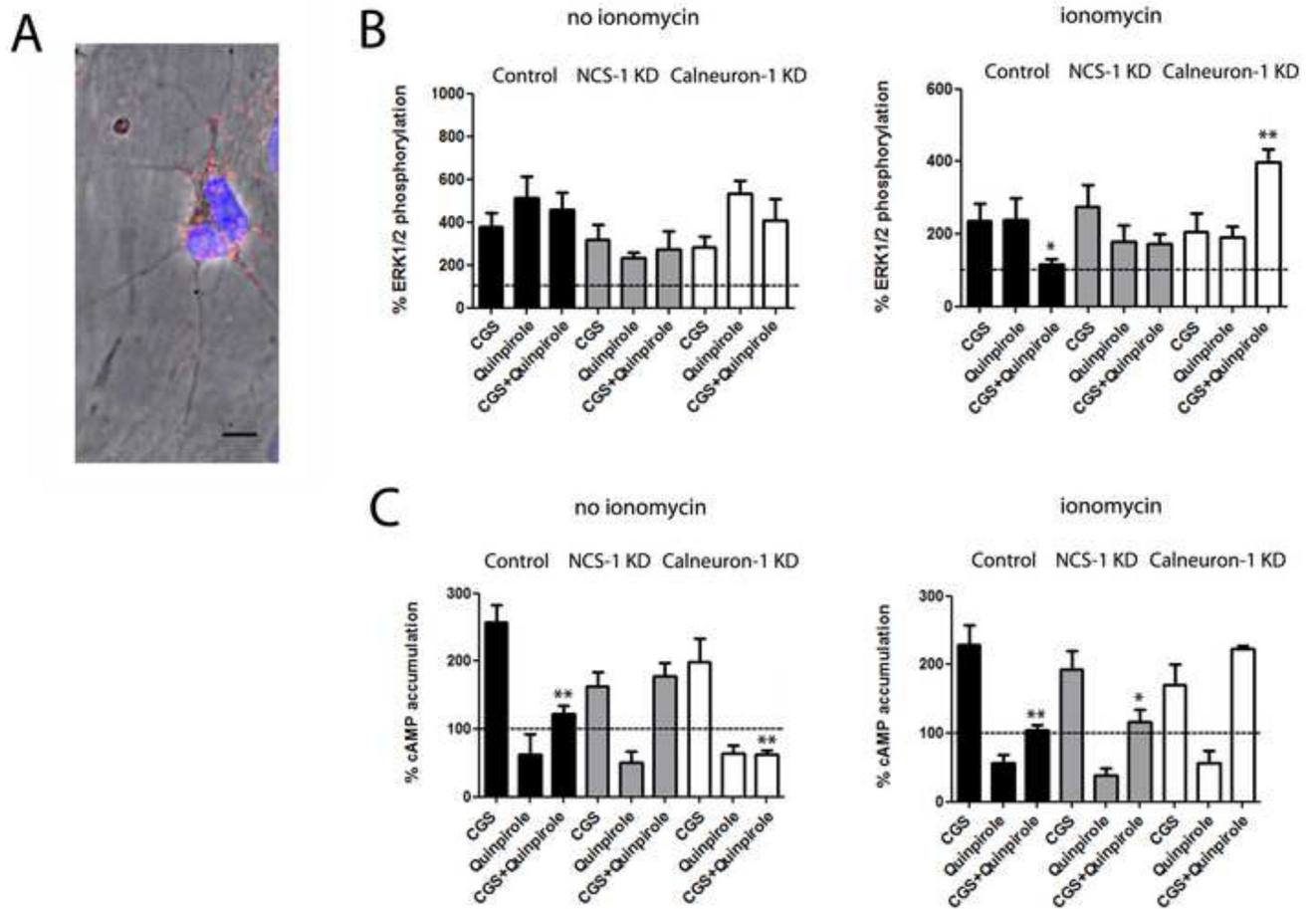


**Figure 5. Modulation by NCS-1 and calneuron-1 of  $A_2A$ R- $D_2$ R heteromer signaling in primary cultures of rat striatal neurons**

**A.**  $A_2A$ R- $D_2$ R heteromers detected by Proximity Ligation Assay (PLA) and confocal microscopy images (superimposed sections) in rat striatal neurons in culture.  $A_2A$ R- $D_2$ R heteromers are seen as red and cell nuclei in blue (Hoesch stain). Scale bars = 20  $\mu$ m.

**B.** ERK1/2 phosphorylation in striatal primary cultures not transfected or transfected with NCS-1 shRNA cDNA (1.5  $\mu$ g; gray bars) or with calneuron-1 shRNA cDNA (1.5  $\mu$ g; white bars) after administration of the  $A_2A$ R agonist CGS 21680 (CGS, 100 nM), the  $D_2$ R agonist quinpirole (1  $\mu$ M) or both, in the absence or presence of ionomycin (left and right graphs, respectively). ERK1/2 phosphorylation levels are expressed as a percentage over basal. **C.** Levels of cAMP in striatal primary cultures not transfected or transfected with NCS-1 shRNA cDNA (1.5  $\mu$ g; gray bars) or with calneuron-1 shRNA cDNA (1.5  $\mu$ g; white bars) after administration of the  $A_2A$ R agonist CGS 21680 (CGS, 100 nM), the  $D_2$ R agonist quinpirole (1  $\mu$ M) or both, in the absence or presence of ionomycin (left and right graphs, respectively). Levels of cAMP after CGS alone or after CGS plus quinpirole are expressed as a percentage over basal; cAMP after quinpirole alone are expressed as percentage of decreases with respect to cAMP induced by forskolin (0.5  $\mu$ M); basal and forskolin-induced cAMP were given as 100% and represented by a dotted line. In **A**, values are expressed as a percentage over basal (100%, dotted line), as means  $\pm$  S.E.M. of 4 to 6 different experiments; one-way ANOVA followed by *post hoc* Dunnett's multiple comparisons: \* $p$  <

0.05 and \*\*\* $p < 0.001$  versus basal; ## $p < 0.01$  versus respective agonist alone. In **B** and **C**, values are means  $\pm$  S.E.M. of 4 to 6 different experiments; one-way ANOVA followed by *post hoc* Dunnett's multiple comparisons: \* $p < 0.05$  and \*\* $p < 0.01$  versus CGS 21680 treatment.

Author Manuscript

Author Manuscript

Author Manuscript

Author Manuscript

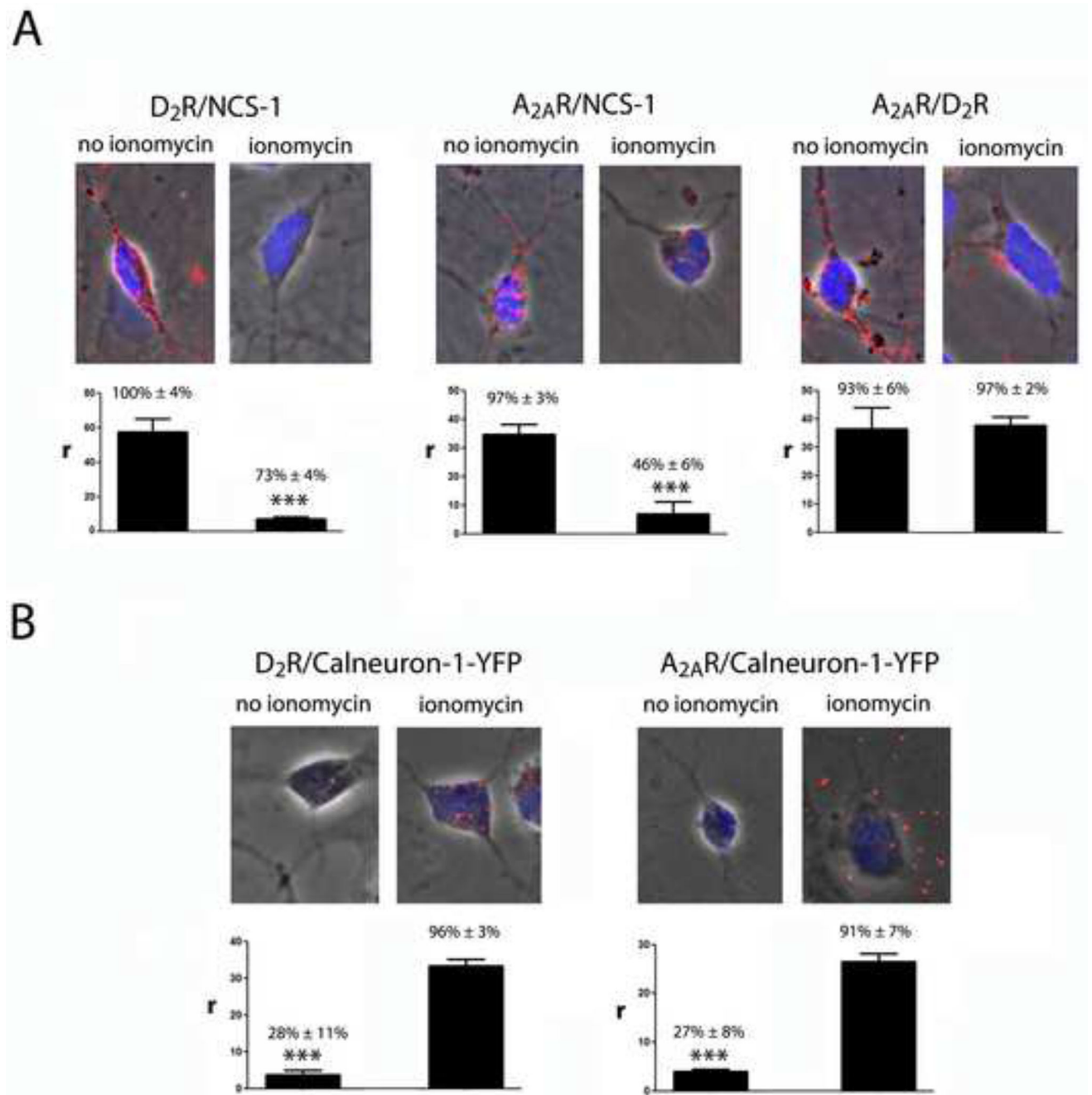


**Figure 6. Interactions of NCS-1 and calneuron-1 with A<sub>2</sub>A<sub>R</sub>-D<sub>2</sub>R heteromers in striatal neurons depend on intracellular Ca<sup>+2</sup> levels**

**A.** Proximity Ligation Assay (PLA) and confocal microscopy images (superimposed sections) in rat striatal neurons in culture, using primary antibodies for D<sub>2</sub>R and NCS-1 (left panels), A<sub>2</sub>A<sub>R</sub> and NCS-1 (middle panels) and A<sub>2</sub>A<sub>R</sub> and D<sub>2</sub>R (right panels), in the absence or presence of ionomycin (1 μM). **B.** Proximity Ligation Assay (PLA) and confocal microscopy images (superimposed sections) in rat striatal neurons in culture transfected with calneuron-1-YFP cDNA (1 μg), using primary antibodies for D<sub>2</sub>R and YFP (left panels), A<sub>2</sub>A<sub>R</sub> and YFP (right panels), in the absence or presence of ionomycin (1 μM). Receptor

heteromers and receptor-Ca<sup>2+</sup>-binding protein complexes appear as red clusters in neurons detected by phase contrast. Scale bars = 20  $\mu$ m. Cell nuclei were stained with Hoesch (blue). The bar graphs represent PLA quantification: *r* values represent number of red spots/cell containing spots and percentage values represent the percentage of cells containing one or more red spots respect to the total number of cells. Data (% of positive cells or *r*) are means  $\pm$  SEM of counts in 20–30 different neurons of three independent preparations. One way ANOVA and followed by Bonferroni *post hoc* test: \*\*\**p* <0.001 compared to no ionomycin (in A) or ionomycin (in B) of *r* values

Author Manuscript

Author Manuscript

Author Manuscript

Author Manuscript

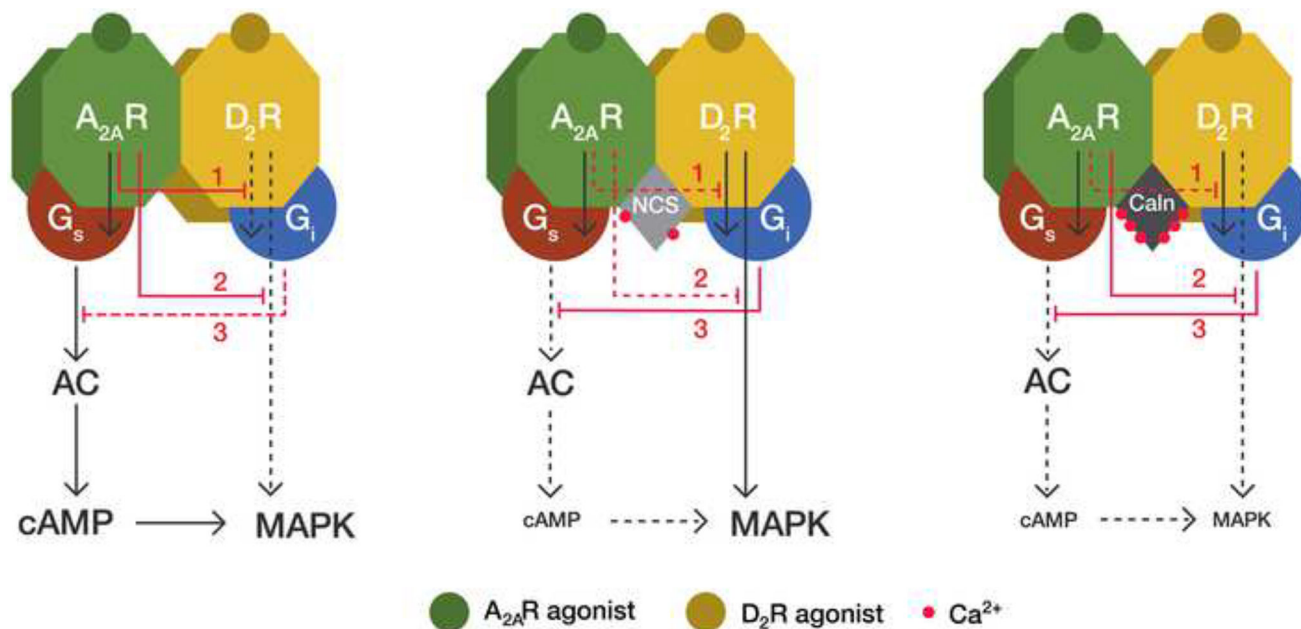


**Figure 7. Model representing the differential role of NCS-1 and calneuron-1 in A<sub>2A</sub>R-D<sub>2</sub>R heteromer signaling**

Depending on the intracellular Ca<sup>+2</sup> levels, the neuronal Ca<sup>+2</sup>-binding proteins NCS-1 (NCS) and calneuron-1 (Caln) exert a differential modulation of A<sub>2A</sub>R-D<sub>2</sub>R heteromer signaling. In the absence of Ca<sup>+2</sup>-binding proteins the D<sub>2</sub>R agonist cannot counteract the ability of the A<sub>2A</sub>R agonist to induce cAMP accumulation (3), due to an allosteric modulation by which A<sub>2A</sub>R activation inhibits D<sub>2</sub>R-mediated G protein-dependent signaling (1). Under these conditions, A<sub>2A</sub>R activation also inhibits the D<sub>2</sub>R agonist-mediated G protein-independent MAPK activation (2). These two allosteric modulations (1 and 2) are absent when NCS-1 binds to the receptor heteromer in the presence of low intracellular Ca<sup>+2</sup> levels. Under these conditions, co-activation of both receptors in the heteromer does not produce cAMP accumulation but still induces MAPK activation. When calneuron-1 binds to A<sub>2A</sub>R-D<sub>2</sub>R heteromer, the allosteric modulation at the level of G protein-dependent signaling (1) is selectively disrupted and the allosteric modulation at the level of G protein-independent signaling (2) is maintained. This results in very low activation of both MAPK signaling and cAMP production upon co-activation of both receptors in the heteromer, since A<sub>2A</sub>R agonist-mediated MAPK activation (which is dependent on AC signaling) is also inhibited (3).